Star Formation in the Galactic Center: SOFIA FIFI-LS Observations of Sgr B1

Jan Simpson (SETI Institute)

With thanks to Sean Colgan, Angela Cotera, Michael Kaufman, and Susan Stolovy

Outline

Ionized gas in the Galactic Center (GC)

Star formation in the GC

Where does Sgr B1 fit into this picture?

SOFIA FIFI-LS Observations of Sgr B1

Where are the stars that produce the excitation?

Summary and Conclusions

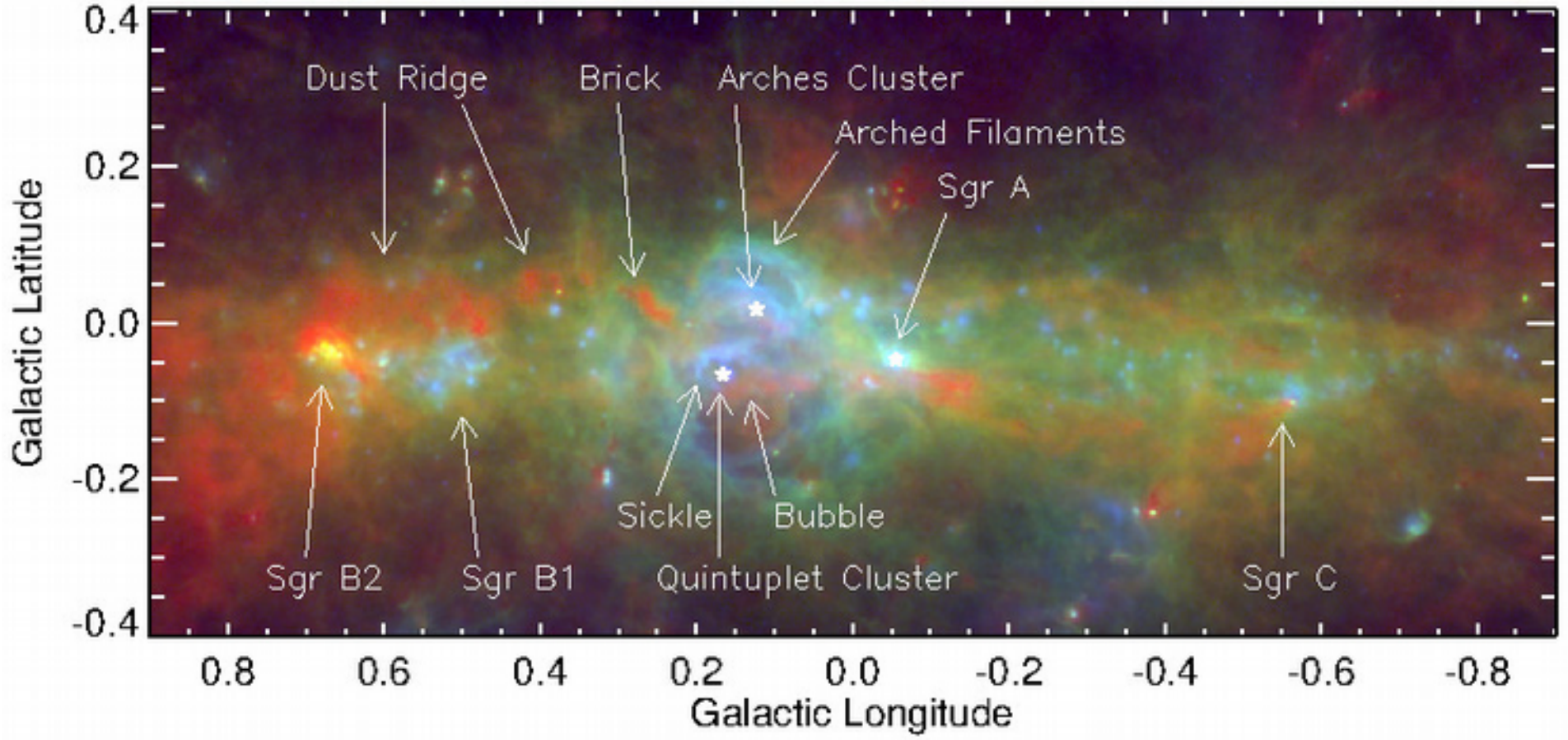

Three-color image of the Galactic Center region, centered on the nuclear cluster Sgr A. H II regions are prominent in the blue (21 μm MSX Band E image from Price et al. 2001) and green (70 μm image from the Herschel Hi-GAL survey, Molinari et al. 2016) images, and the cold molecular clouds are conspicuous in the red image (500 μm image, also from the Hi-GAL survey).

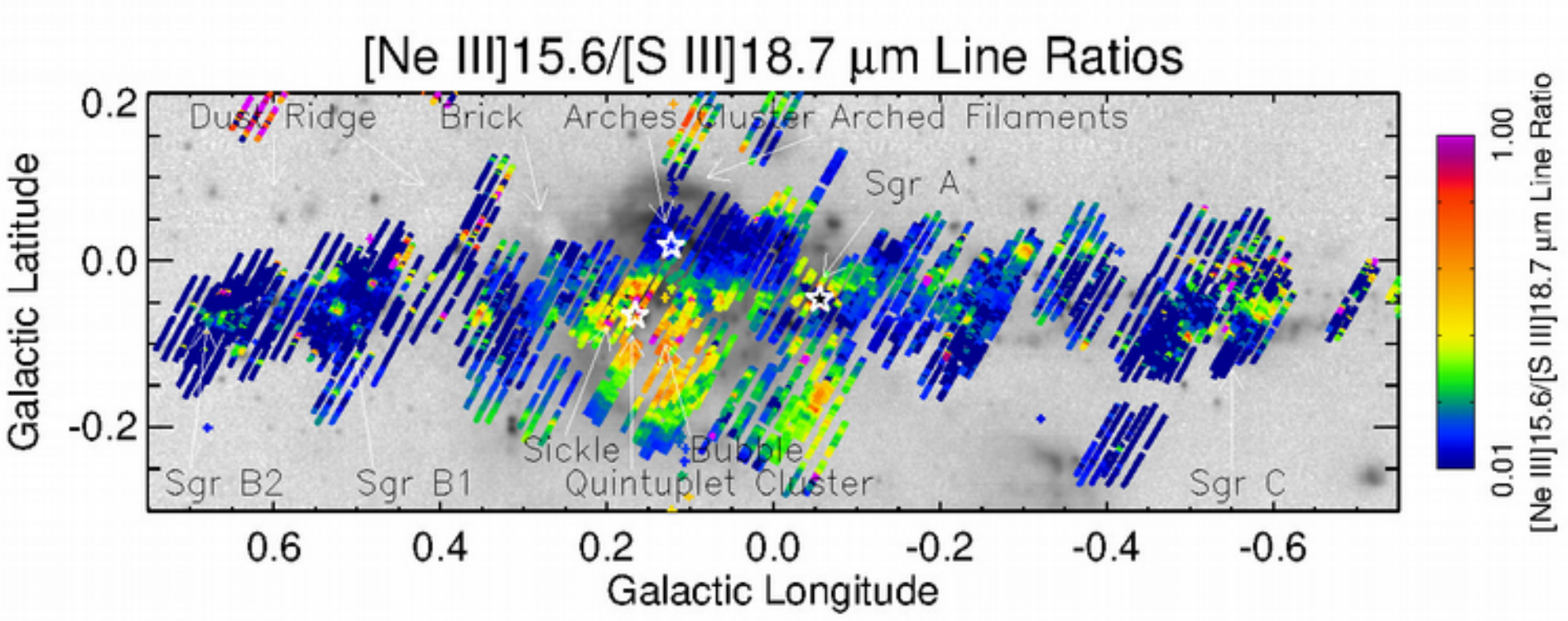

Ratio of the [Ne III] 15.6 µm line divided by the [S III] 18.7 µm line from Simpson (2018). The spectra were taken with the Spitzer Infrared Spectrograph. The generally low excitation (ratio < 0.2) means either exciting stars with T_{eff} < 35,000 K (or Starburst99 age > 2.5 Myr) or a very dilute radiation field due to multi-parsec distance from stars to gas. Bright magenta dots are either shocks or candidate PNe. The Radio-Arc Bubble also has a substantial shock contribution to its excitation. The source at longitude ~ 0.65 is not Sgr B2, which has too high extinction to be detected at mid-infrared wavelengths, but is foreground diffuse gas.

Star Formation in the Galactic Center

The current paradigm favors the idea that molecular clouds in orbit around Sgr A* are compressed as they pass pericenter, thereby enabling star formation.

The observational result is that the ages of the young star clusters are a function of position along the orbit.

These ideas have been elucidated by
J. M. D. Kruijssen, S. N. Longmore, A. T. Barnes, J. D. Henshaw, J. M. Rathborne, and others (see the last slide for references).

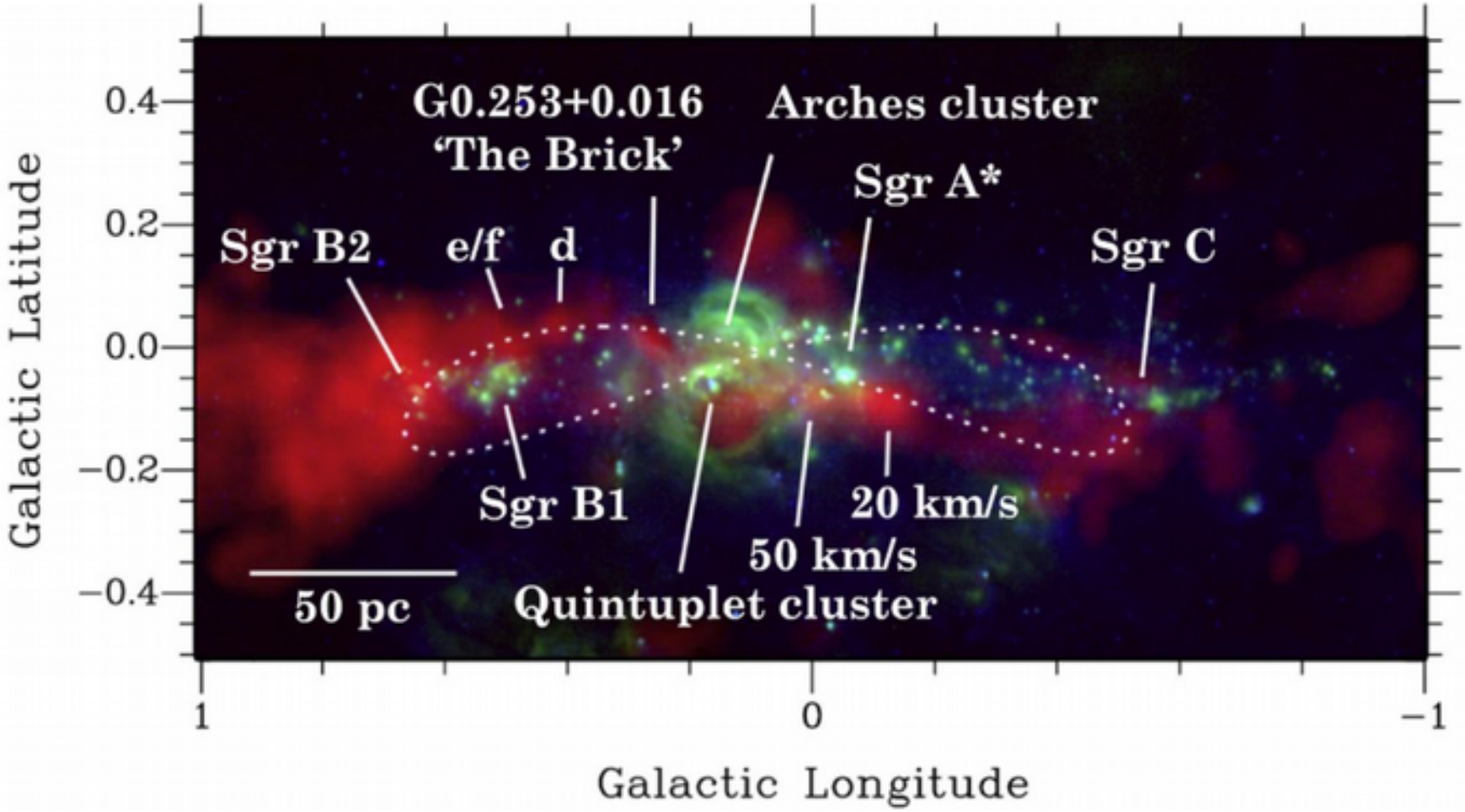

Three-color image of the GC from Kruijssen et al. (2016). The dotted line shows the 100 pc twisted elliptical ring of molecular clouds first described by Molinari et al. (2011).

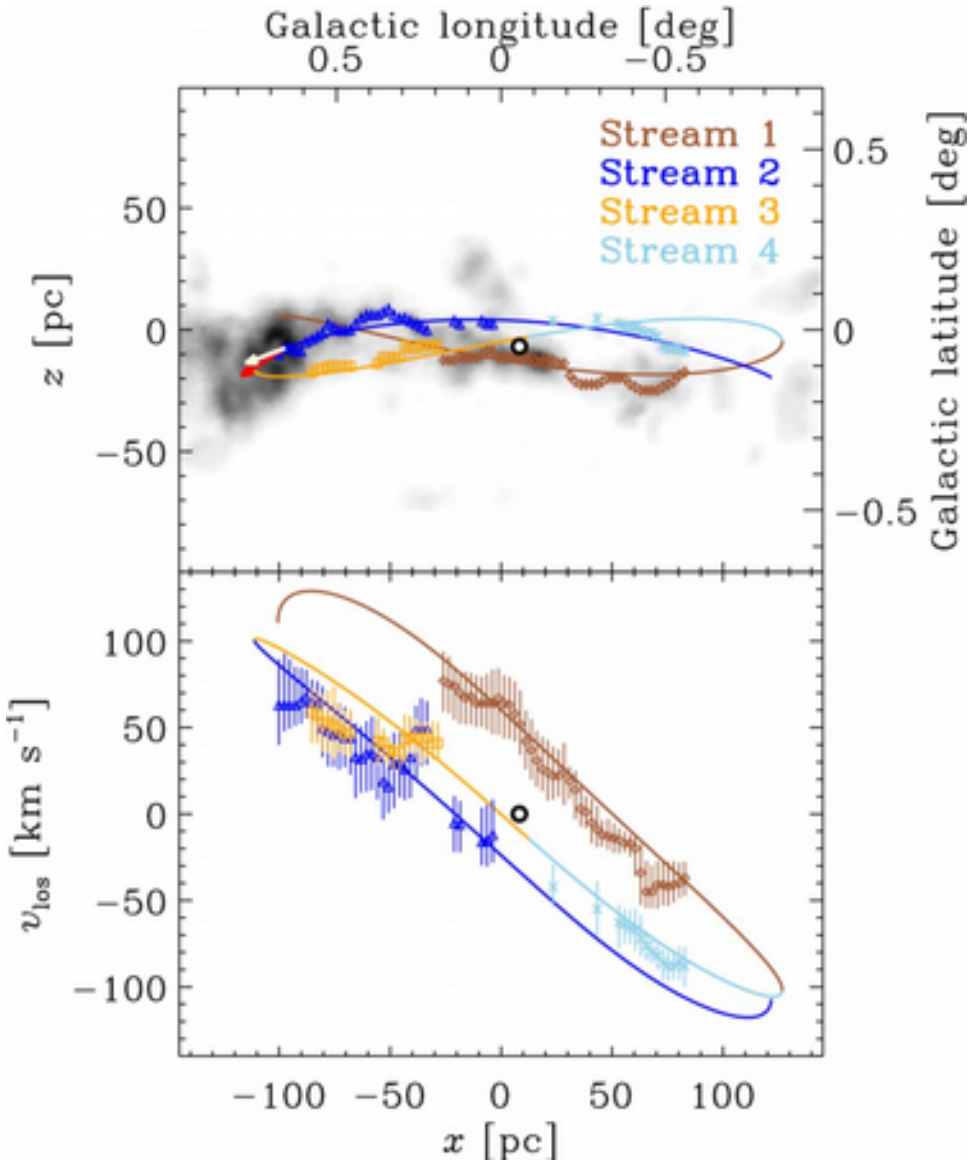

Kruijssen et al. (2015) showed that the elliptical ring of molecular clouds could be better fit by four streams of gas in the GC. Starting at the far right, Stream 2 approaches the earth passing Sgr A* (the open black circle); at the far left (the red and white arrows), it transitions to Stream 3 which returns on the far side, becoming Stream 4 as it passes behind Sgr A*; the stream transitions to Stream 1, which again passes in front of Sgr A* after making one complete orbit about the GC.

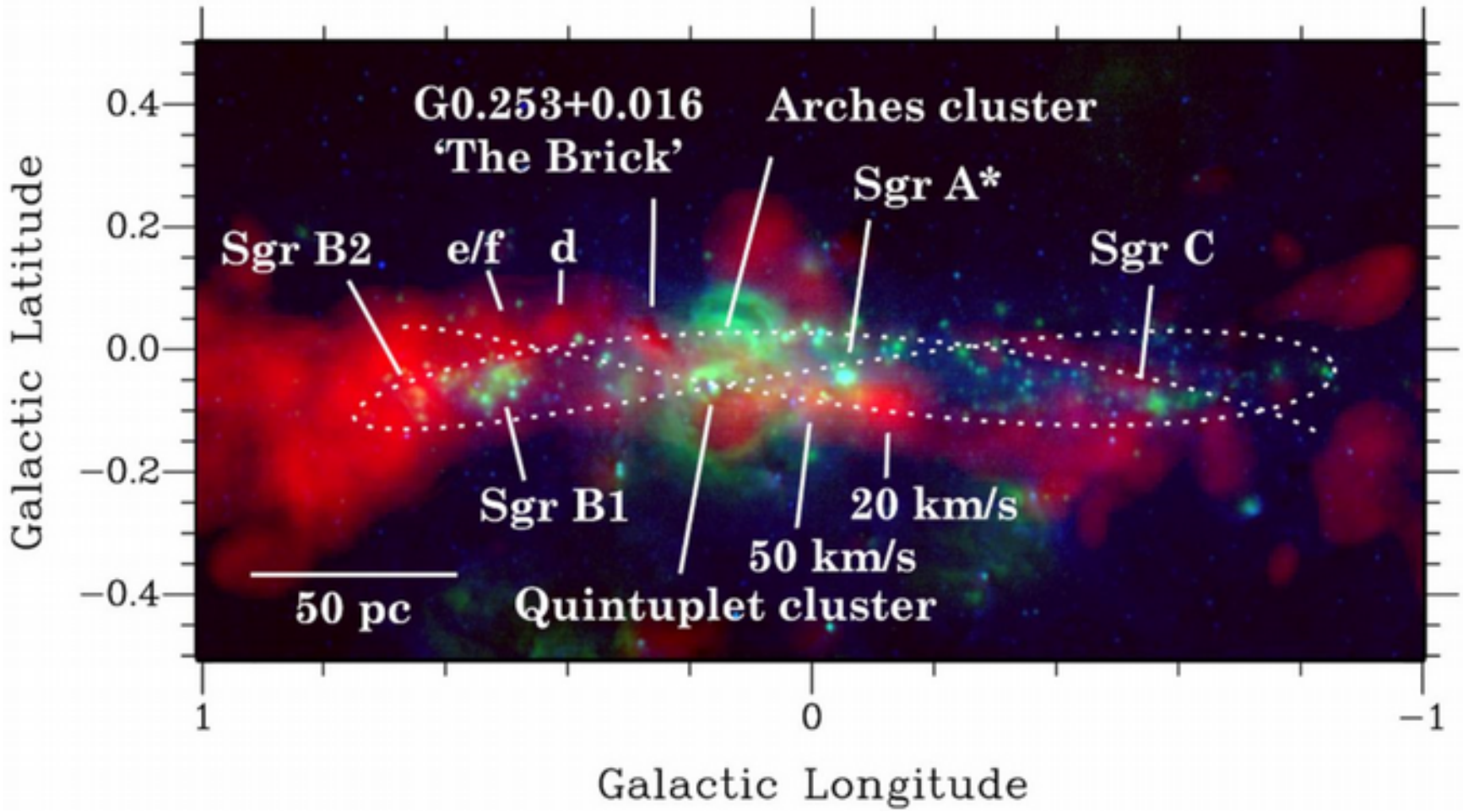

Molecular cloud orbits in the GC, from Kruijssen et al. (2015).

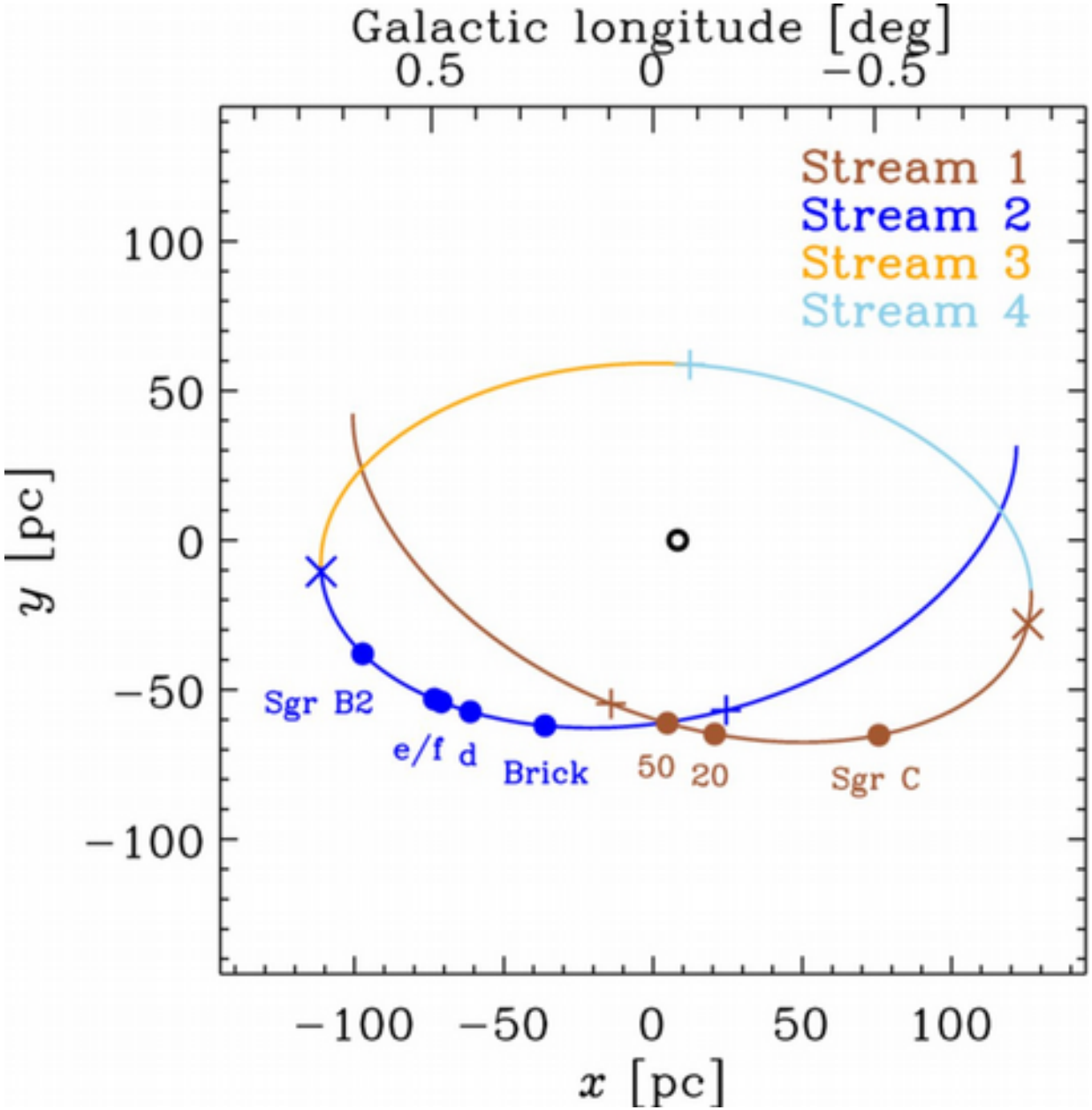

A top-down view of the four streams from Kruijssen et al. (2015), showing the order of time from pericenter (crosses) and apocenter (x's). Sources with no current massive star formation are the Brick (Rathborne et al. 2015), and molecular clumps d, e, and f. Some of the most active massive star formation in the Galaxy is found in Sgr B2 (e.g., Ginsburg et al. 2018). Sgr C and the 20 and 50 km/s molecular clouds are found on Stream 1.

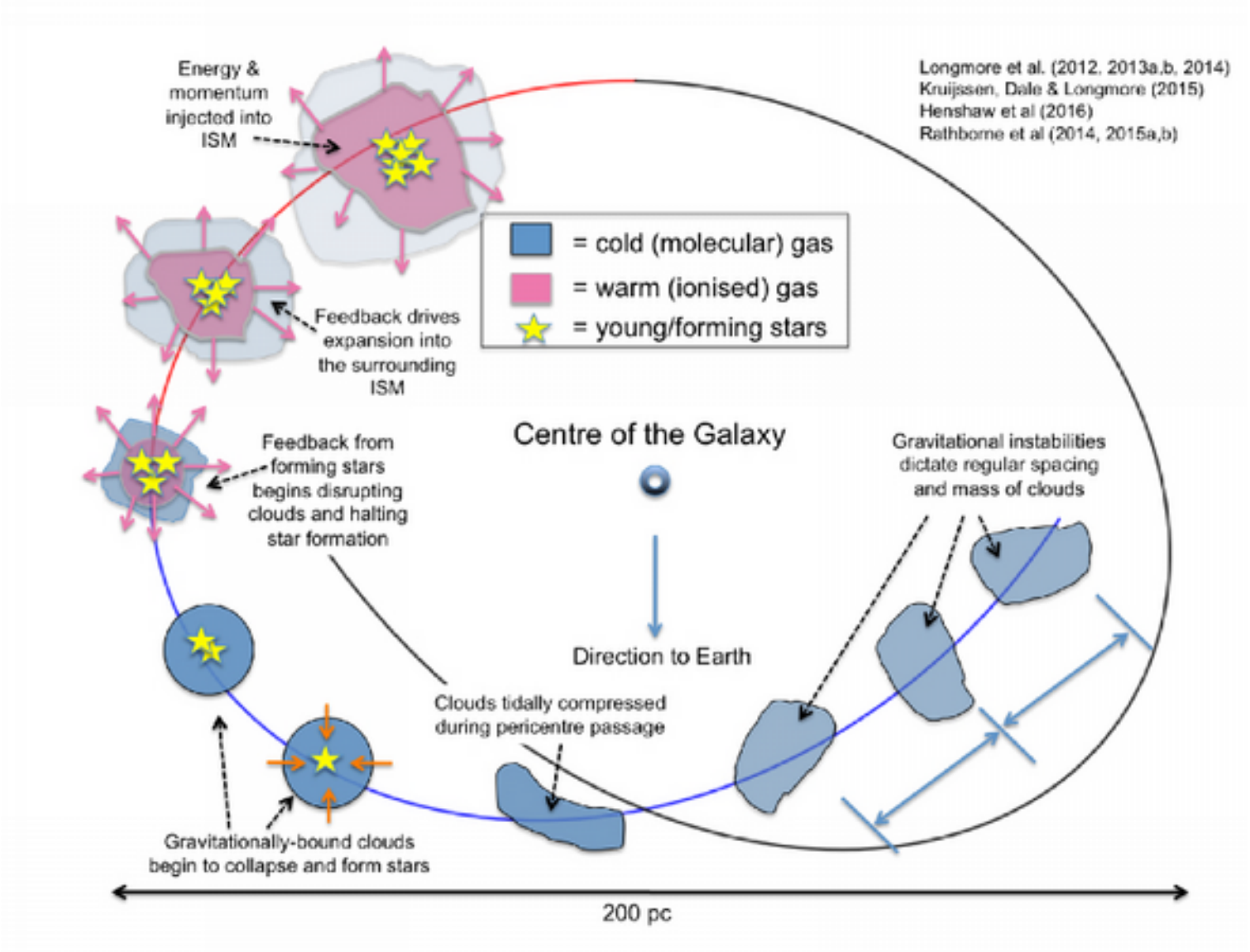

Cartoon of the GC star formation scenario from Longmore et al. (2015).

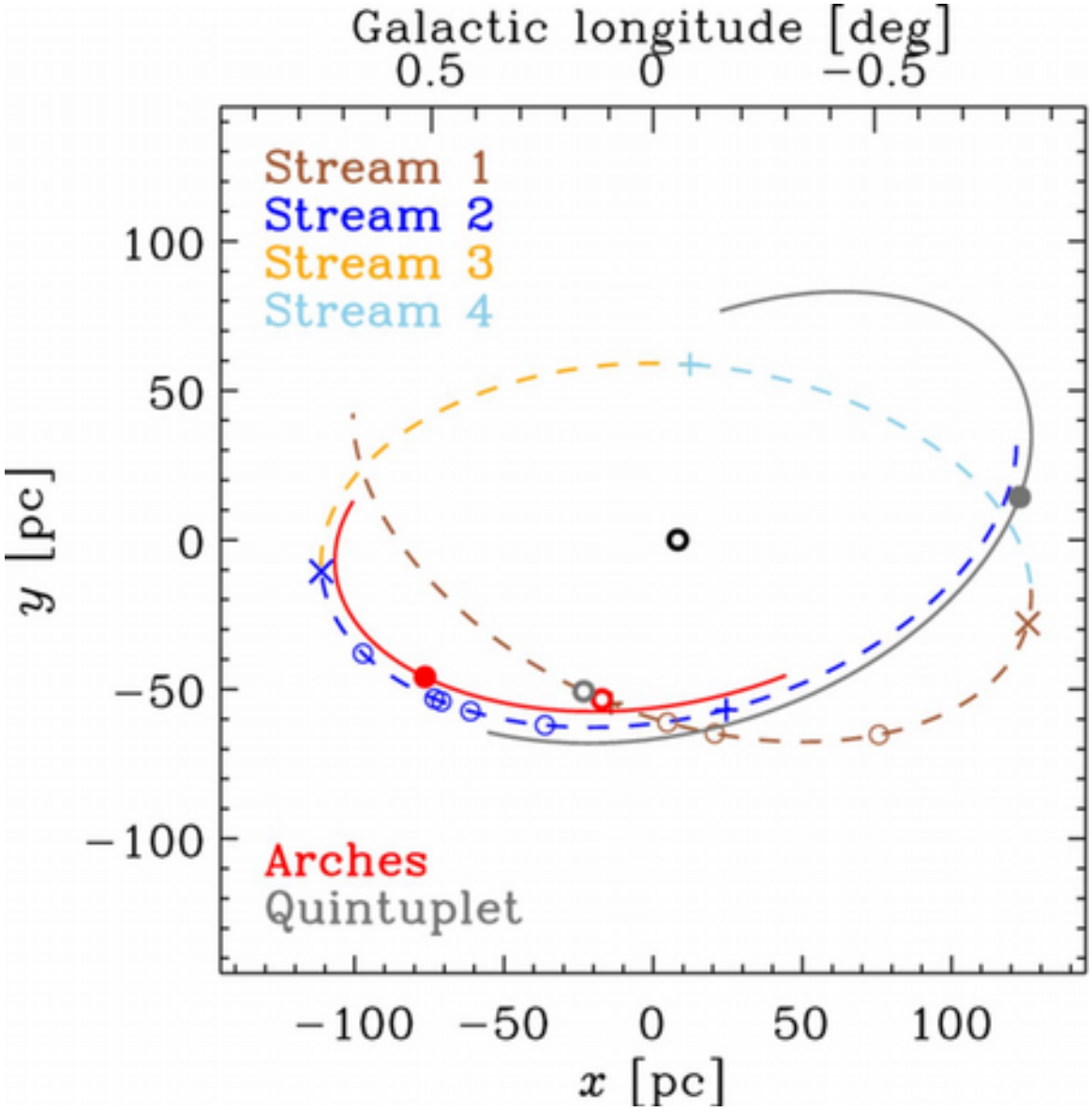

Kruijssen et al. (2015) also plot the origin (solid dots) and current positions (open circles) of the Arches and Quintuplet Clusters. Each cluster has already made approximately one complete orbit around Sgr A* (black circle), taking approximately 4 Myr.

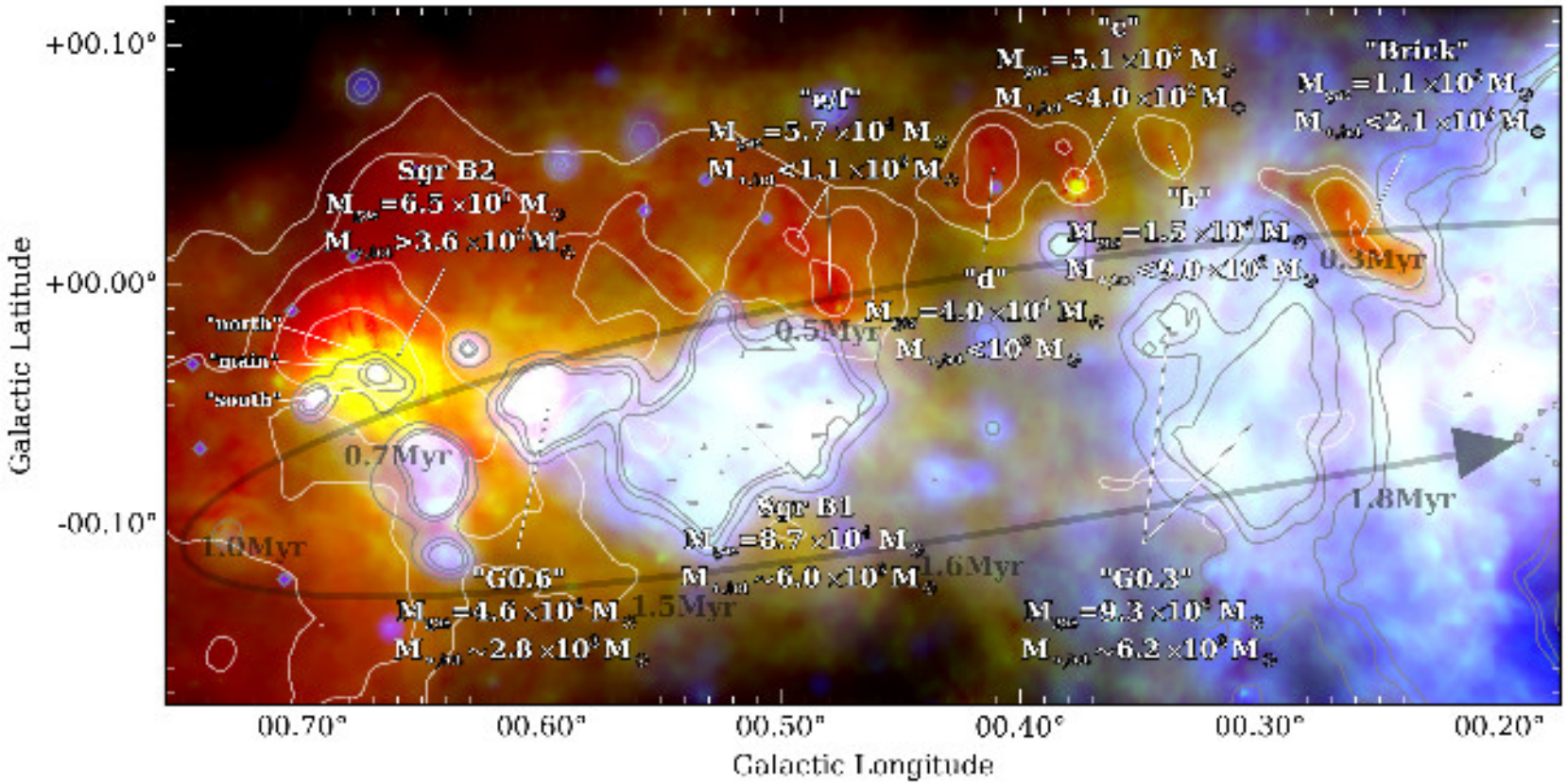

The young molecular clouds and the luminous H II regions Sgr B2 and Sgr B1 shown on their orbital path, from Barnes et al. (2017).

Sgr B1, however, does not fit very well into this scenario.

Models of H II regions that fit the observed Spitzer mid-infrared IRS spectra of the oxygen, neon, silicon, and sulfur all have ionizing spectral energy distributions corresponding to stellar clusters of age ~ 4.6 Myr (Simpson 2018), not at all the 1.5 Myr age of the orbital position (Barnes et al. 2017).

Although it lies just beyond Sgr B2 on the orbital path, the radio emission has no compact components (unlike Sgr B2, Ginsburg et al. 2018), and its mostly extended features give the appearance of an evolved H II region (Mehringer et al. 1992).

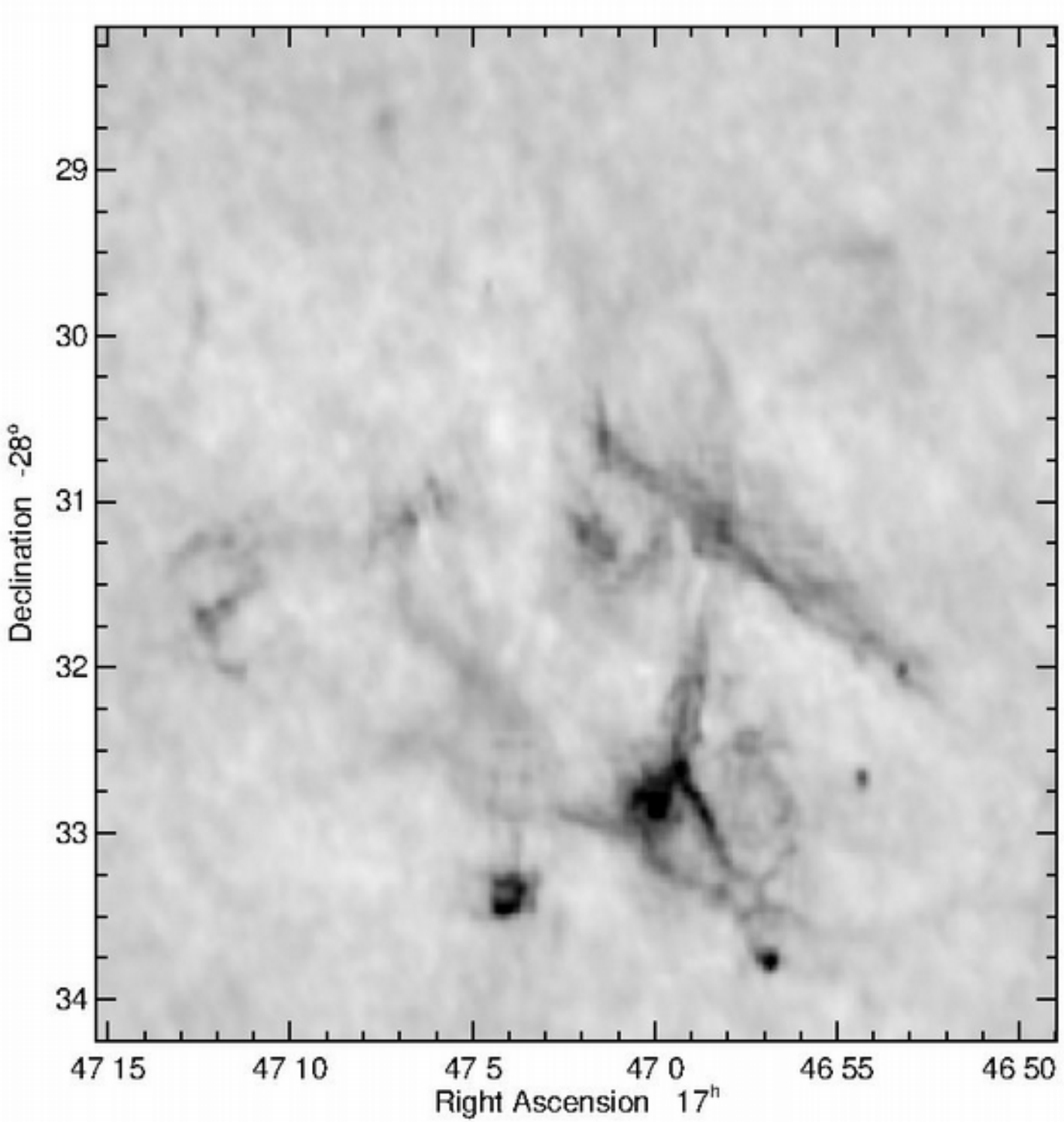

8.4 GHz VLA image of Sgr B1 from Mehringer et al. (1992).

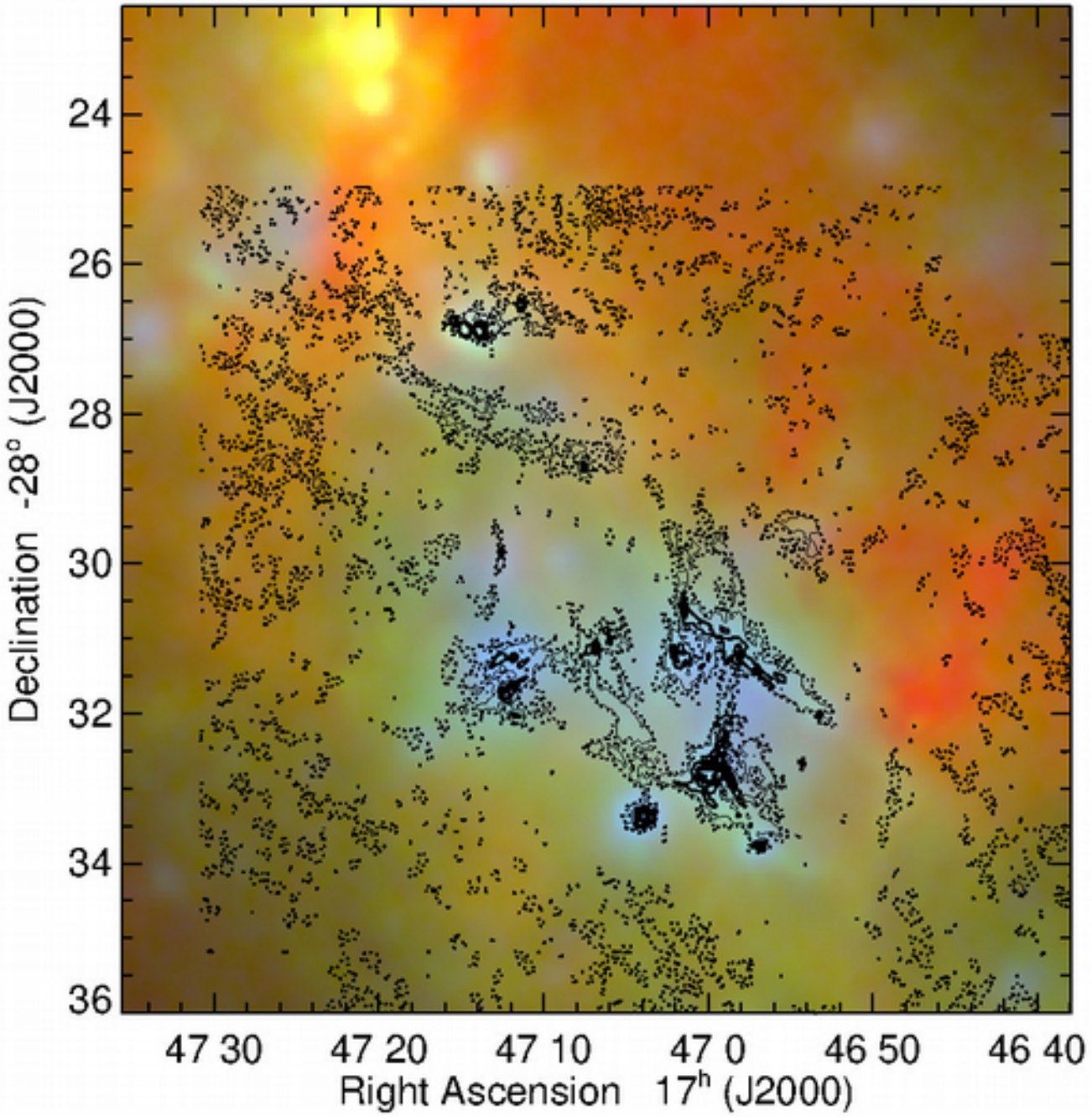

The Sgr B region from the combined 3-color MSX and Herschel image, with the radio contours from Mehringer et al. (1992) overlaid. The highly extincted Sgr B2 is the yellow cluster of sources at the top.

Sgr B1 is found in a hole in the molecular cloud distribution (which is probably foreground, as seen in the greater extinction and absorption lines at the redder positions).

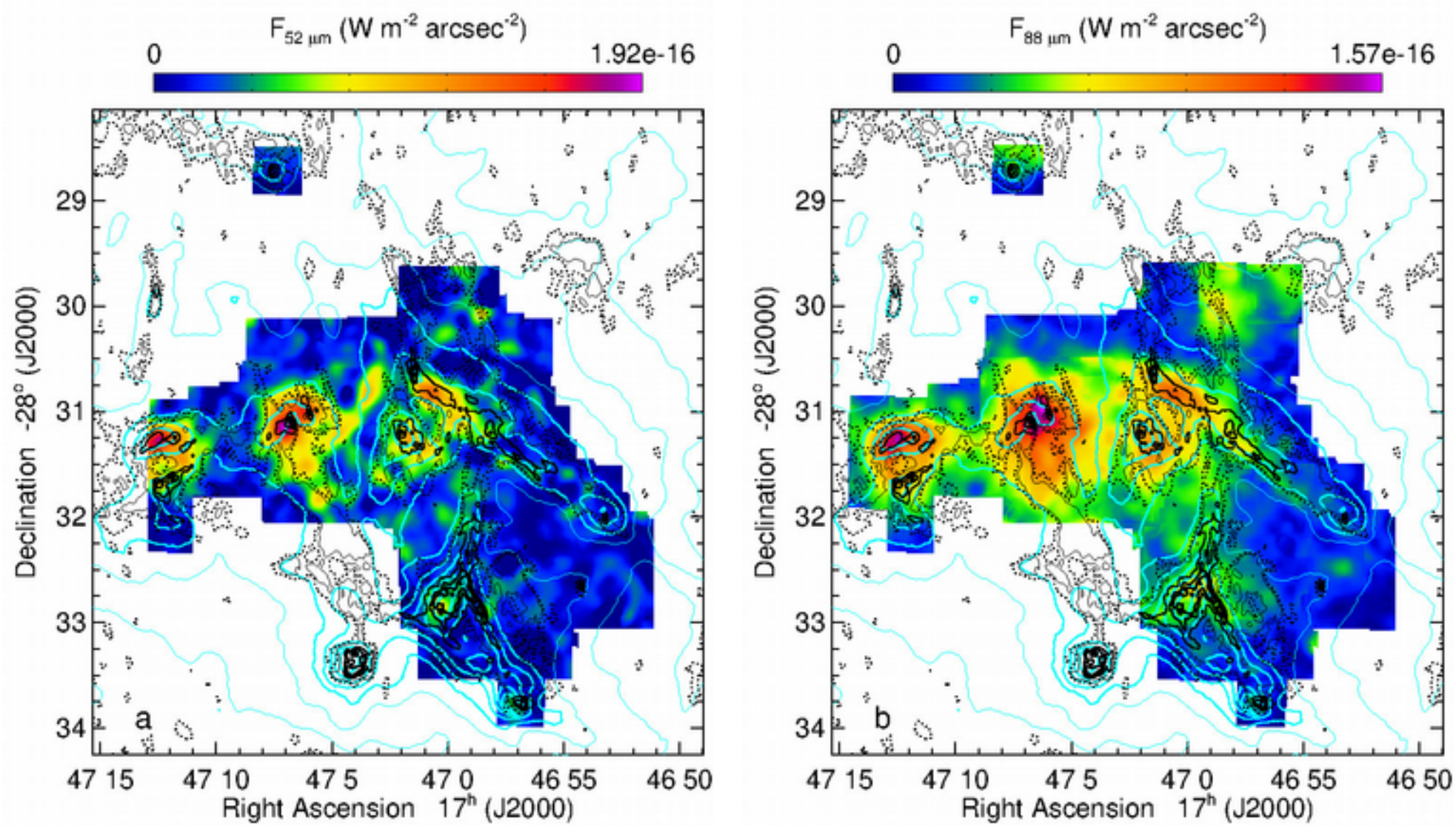

Maps of the [O III] 52 and 88 μm line intensities from SOFIA FIFI-LS observations taken in July 2016 and 2017. The black contours are the 8.4 GHz radio intensities and the cyan contours are the 70 μm Herschel PACS intensities. Figure from Simpson et al. (2018).

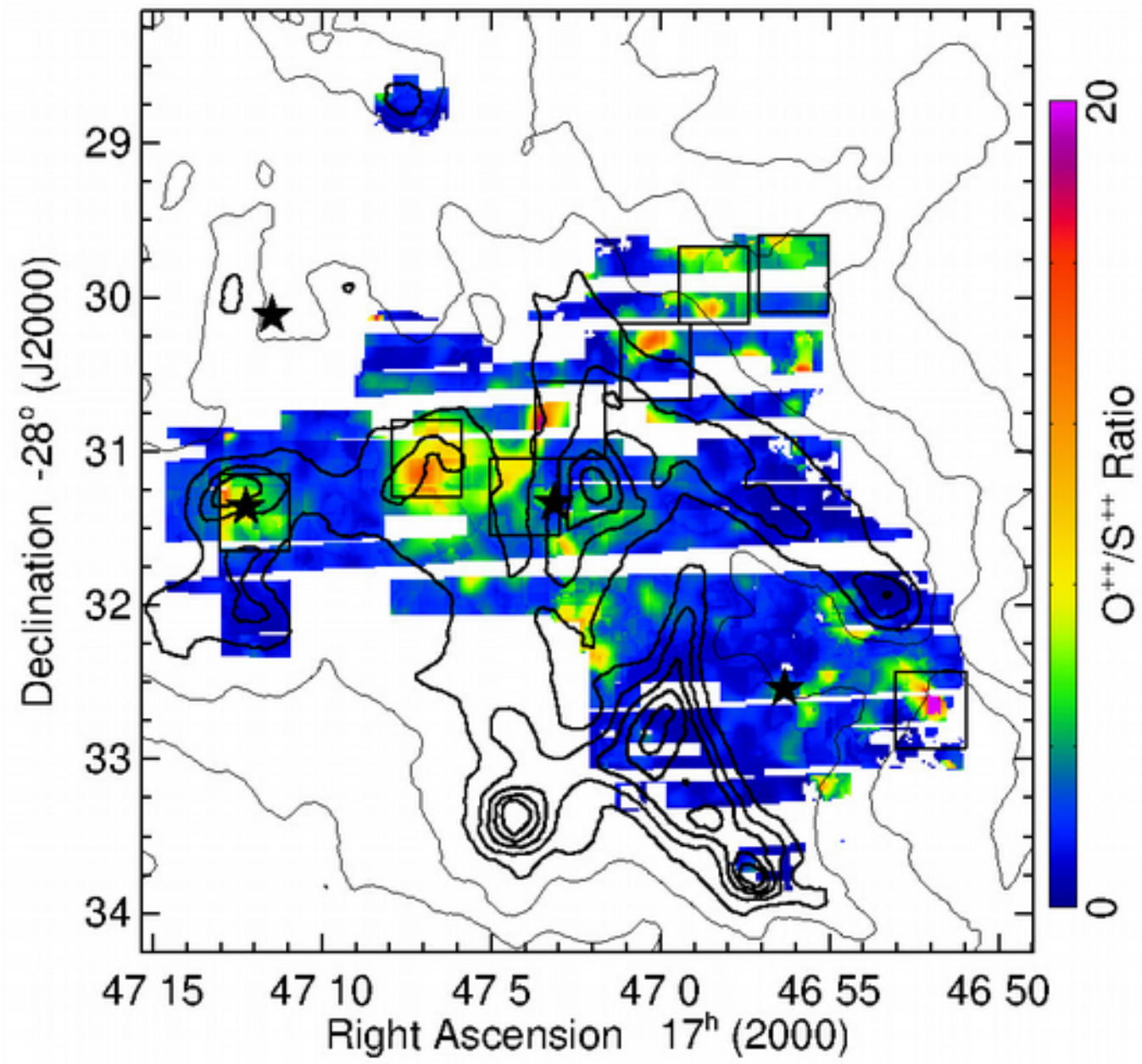

The measured O++/S++ ratio in Sgr B1 from Simpson et al. (2018). We used the [O III] 52/88 μm line ratio to determine the electron density, and then added the Spitzer [S III] line measurements from Simpson (2018, 2019) to estimate the excitation.

The black boxes mark regions of noticeably higher excitation (although not very high).
Note that the excitation does not correlate with the contour peaks (Herschel 70 μm).

The black stars are the WR and O supergiants measured by Mauerhan et al. (2010).

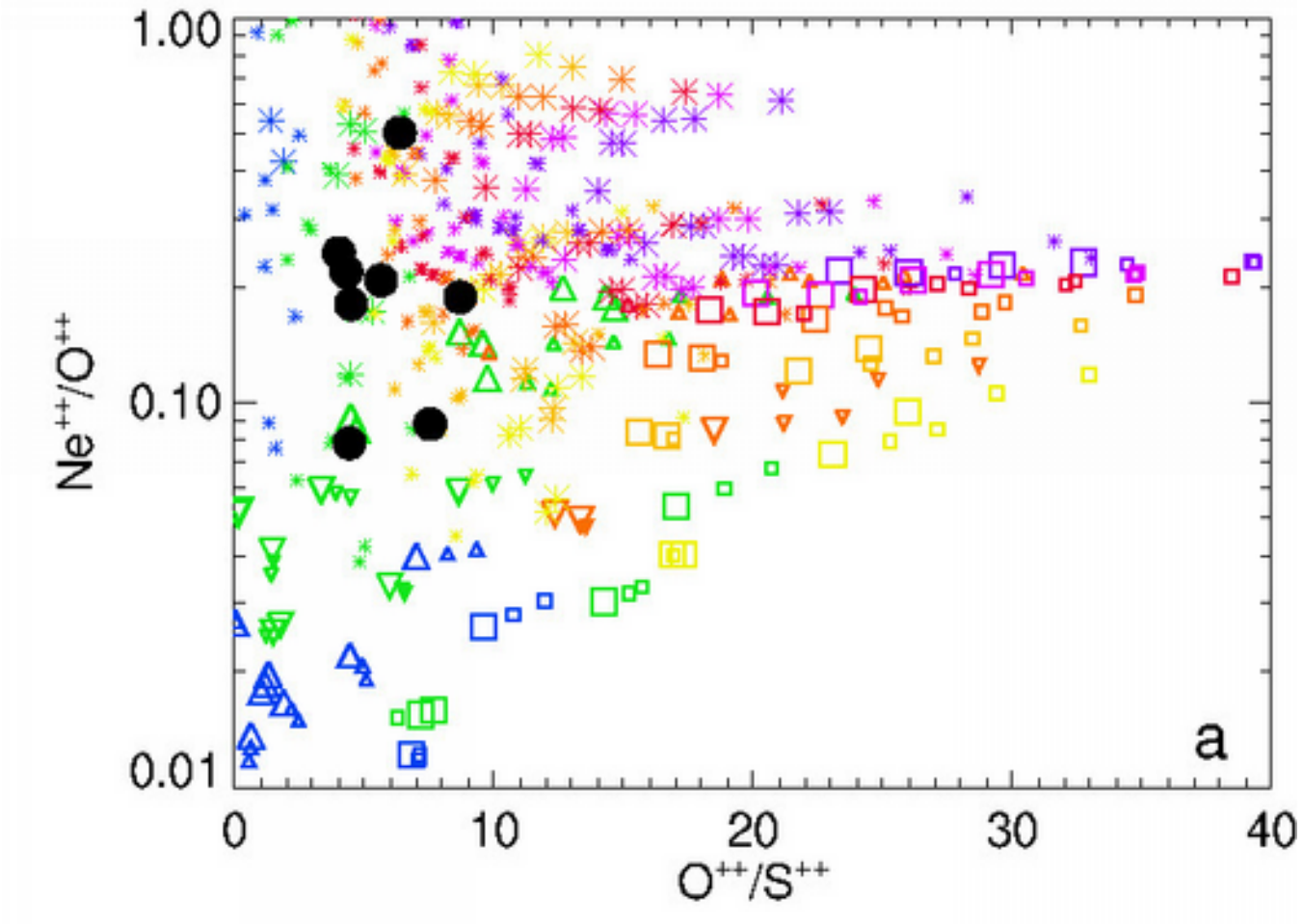

The black dots are the integrated abundance ratios from the higher excitation positions marked in the previous slide. The colored points are H II region models computed for various densities, radii, and filling factors with stellar SEDs marked by color. Blue and green are Teff < 35,000 K or age > 4.5 Myr; yellow to red are hotter or younger, but only the magenta and purple dots have ages as young as 1.5 Myr that would correspond to Sgr B1's orbital position. Figure from Simpson et al. (2018).

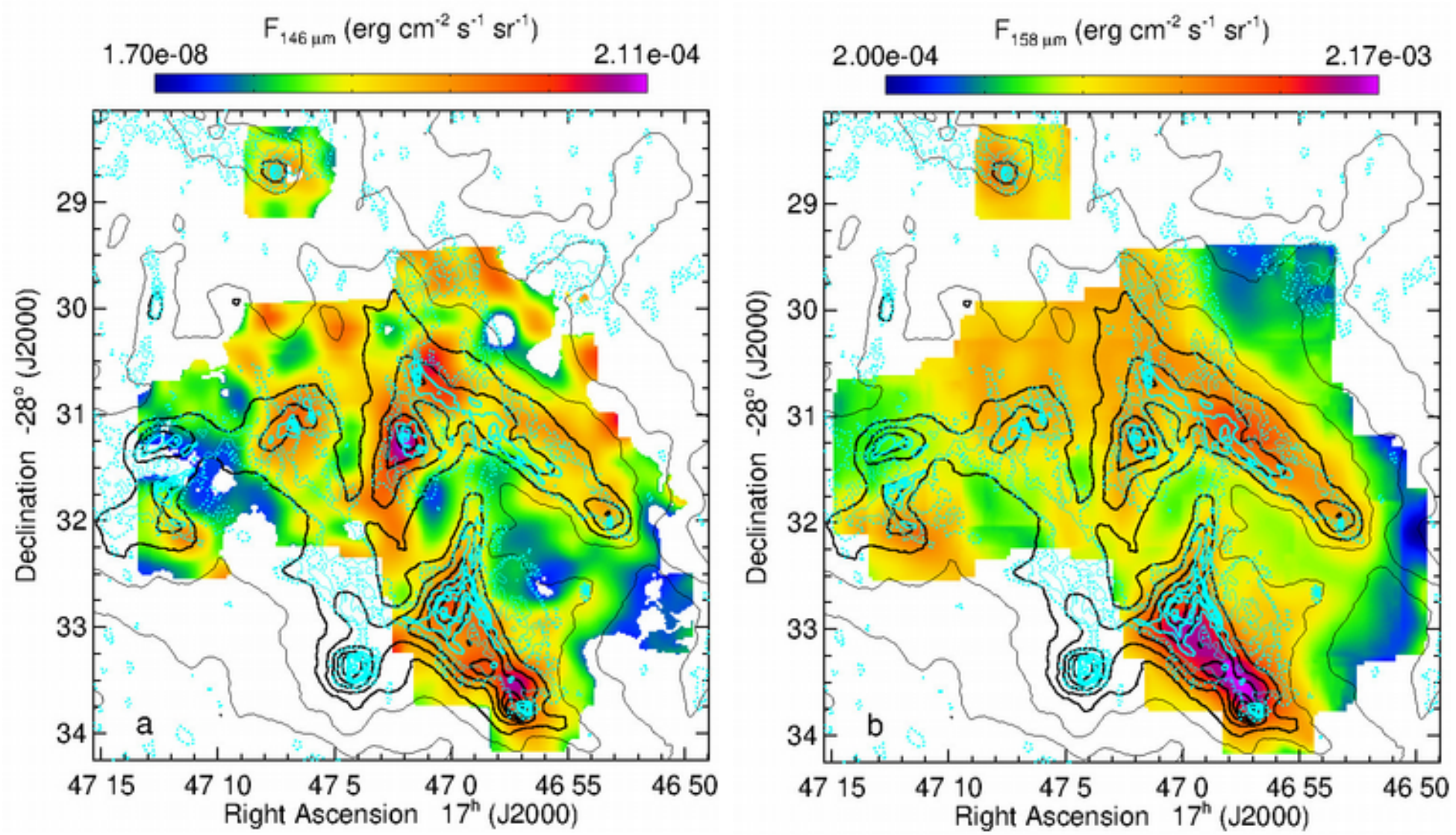

Intensities of the [O I] 146 μm and [C II] 158 μm photodissociation (PDR) lines from measurements made with FIFI-LS at the same times as the [O III] line measurements. Note that these line intensities have much better agreement with the Herschel 70 μm intensities (black contours) and the 8.4 GHz VLA intensities (cyan contours) than the [O III] line intensities.

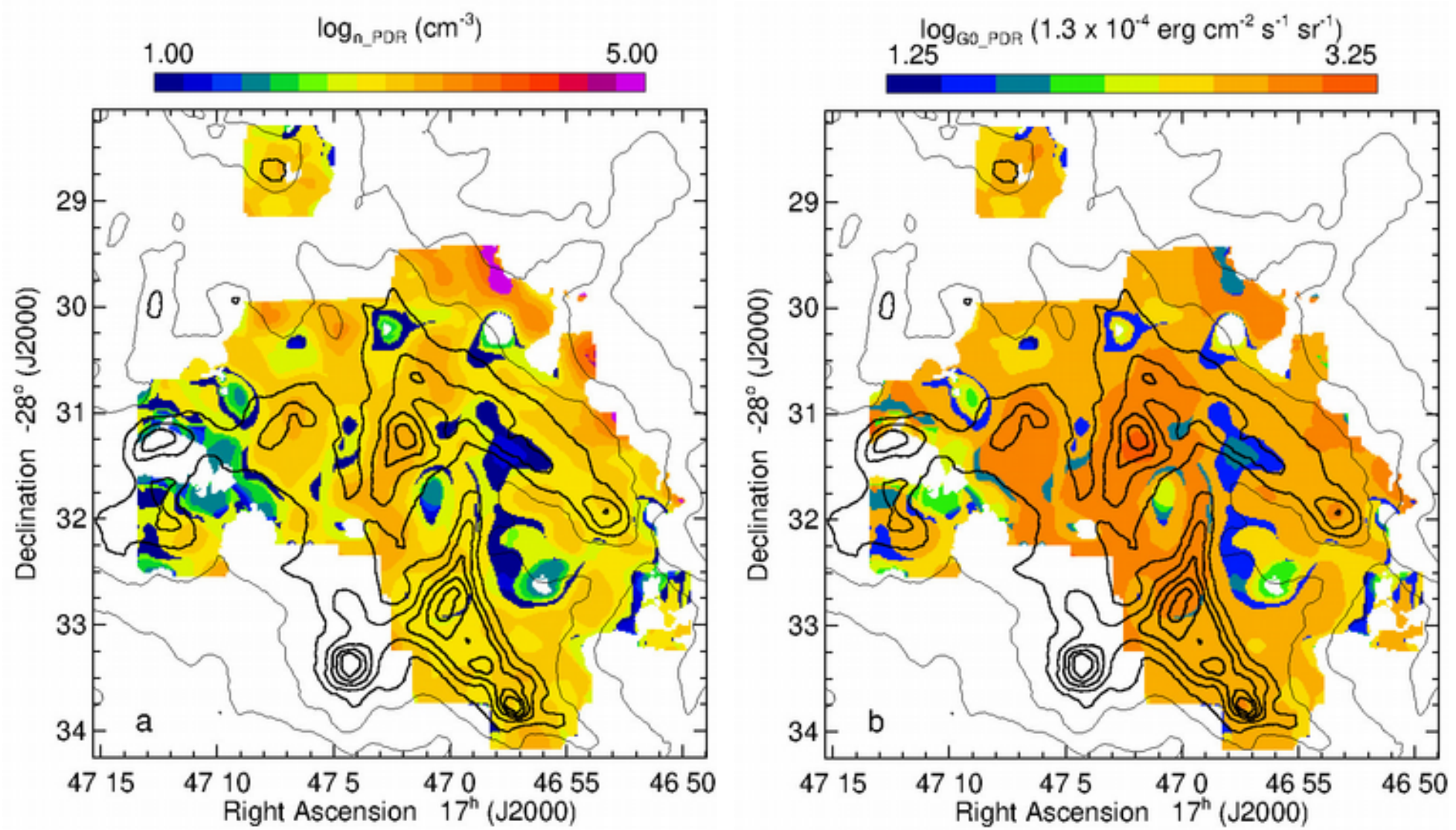

Estimates of the PDR proton density n and incident flux G0, made using the online PDR Toolbox (Kaufman et al. 2006; Pound & Wolfire 2008). The proton densities (500-1000 cm-3) agree well with the electron densities from the [O III] lines and the regions with the highest G0 agree with the regions of higher excitation. We conclude that the same stars that are ionizing the H II region are heating and ionizing the PDR.

In Sgr B1, the more highly excited gas (O^{++}) is not correlated with either radio emission (VLA) or warm dust (Herschel 70 μm), although the neutral gas ([O I]) and low ionization gas (C^{+}) is.

Except for the WR and OI stars, no stars are seen to cluster in or near the ionized gas. In fact, since the more highly ionized regions are dispersed like the gas and dust, we suggest that the exciting stars are also dispersed throughout the region.

There is a significant age difference between the time the Sgr B1 gas last passed the Sgr A* pericenter (about 1.5 Myr) and the estimated age of the ionizing stars that produce the best fits to the forbidden line observations of Sgr B1 (about 4 Myr).

A possible resolution to this conundrum that the exciting stars did not form within the gas of Sgr B1 but instead formed on a previous passage around Sgr A. This resolution would allow the gas of Sgr B1 to still be associated with Sgr B2, as seems likely given the radial velocity structure seen in both sources.

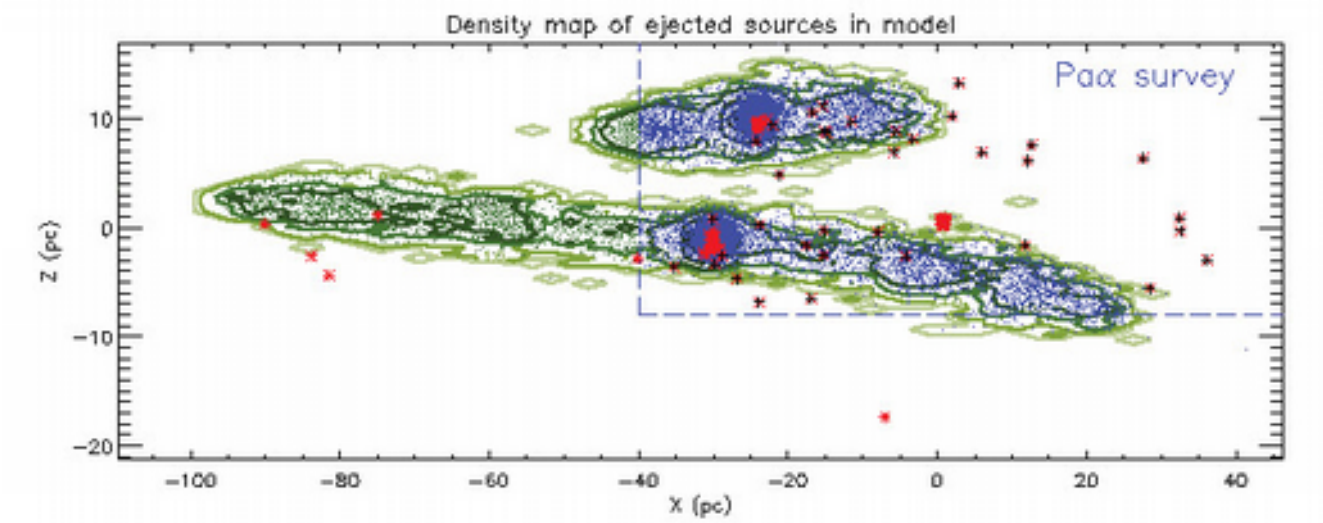

Habibi et al. (2014)

Because of the strong tidal shear in the GC, stars escape readily from even compact star clusters (e.g., Portegies Zwart et al. 2002). Habibi et al. (2014) modeled the escape of stars from the Arches (upper) and the Quintuplet (lower) clusters seen in this figure. In the figure, x is distance (proportional to Galactic longitude) from Sgr A* and z is Galactic latitude from Sgr A*. The red asterisks at the left are the locations of the WR stars in Sgr B (not plotted are the two O4-6I supergiants; Mauerhan et al. 2010).
We suggest that the stars exciting Sgr B1 are either escapees from the Quintuplet Cluster or are the remnants of another ~4 Myr old cluster in the process of dispersing.

Summary and Conclusions

The GC contains 3 massive clusters, 5 luminous H II regions but only 1 region currently actively forming massive stars (Sgr B2)

The GC excitation is generally low, with exceptions for shocked gas (plus some foreground candidate PNe)

Line mapping with SOFIA FIFI-LS combined with mid-IR line measurements (e.g., Spitzer) informs us on the past history of GC star formation

Sgr B1 is probably excited by some massive stars that formed in a separate cluster that is now dispersed (or dispersing, if the stars are from the Quintuplet or Arches clusters)

References

Barnes, A. T., et al. 2017, MNRAS, 469, 2263
Ginsburg, A., et al. 2018, ApJ, 853, 171
Habibi, M., Stolte, A., & Harfst, S. 2014, A&A, 566, A6
Henshaw, J. D., Longmore, S. N., & Kruijssen, J. M. D. 2016, MNRAS, 463, L122
Kaufman, M. J., Wolfire, M. G., & Hollenbach, D. J. 2006, ApJ, 644, 283
Kruijssen, J. M. D., Dale, J. E., & Longmore, S. N. 2015, MNRAS, 447, 1059
Longmore et al., 2015, in Conditions and Impact of Star Formation, eds. R. Simon, R. Schaaf, & J. Stutzki, EAS Publications series, 75-76, 43
Mauerhan, J. C., et al. 2010, ApJ, 710, 706
Mehringer, D. M., et al. 1992, ApJ, 401, 168
Molinari, S., et al. 2011, ApJ, 735, L33
Molinari, S., et al. 2016, A&A, 591, A149
Pound, M. W., & Wolfire, M. G. 2008, in ADASS XVII, ASP Conf Ser, Vol 394, 654 http://dustem.astro.umd.edu/pdrt
Price, S. D., et al. 2001, AJ, 121, 2819
Rathborne, J. M., et al. 2015, ApJ, 802, 125
Simpson, J. P. 2018, ApJ, 857, 59; Erratum 2019, ApJ, 870, 140
Simpson, J. P., et al. 2018, ApJ, 867, L13